

Ligand effects on the structures of $\text{Rh}_6(\text{CO})_{15}\text{L}$ clusters[†]

David H. Farrar,^{*a} Elena V. Grachova,^b Alan Lough,^a Charles Patirana,^a Anthony J. Poë^a
and Sergey P. Tunik^b

^a Department of Chemistry, University of Toronto, 80 St. George Street, Toronto, Ontario, M5S 3H6, Canada

^b St. Petersburg University, Department of Chemistry, Universitetskii pr. 2, St. Petersburg, 198904, Russia

Received 11th December 2000, Accepted 1st May 2001

First published as an Advance Article on the web 18th June 2001

The crystal and molecular structures of the hexarhodium carbonyl clusters $\text{Rh}_6(\text{CO})_{15}\text{L}$ ($\text{L} = \text{P}(\text{OPh})_3$, **1**; $\text{P}(4\text{-XC}_6\text{H}_4)_3$, ($\text{X} = \text{CF}_3$, **2**; Cl , **3**; F , **4**; OMe , **5**); $\text{P}(\text{tBu})_3$, **6**; Me_2SO , **7**; MeCN , **8**; C_8H_{14} , **9**) have been determined by single crystal X-ray crystallography. Redetermination of the structure of the parent $\text{Rh}_6(\text{CO})_{16}$ cluster, **10**, has also been performed and all the results are compared with those for the rather disparate group of monosubstituted derivatives reported earlier. The structures all relate closely to that of the parent which has an octahedral array of Rh atoms with four opposite faces triply bridged by CO ligands. Each Rh atom also has two terminal CO groups attached. The substituents simply replace one of the terminal COs. A group of ligands, comprised of the P-donors and cyclooctene, all show distortions with a high degree of stereoselectivity in the vicinity of the substitution site, and demonstrate the significantly local character of the effect. The effects on the terminal CO groups are mainly limited to the CO attached to the substituted Rh atom for which there is a clear decrease in the Rh–CO distance and a smaller lengthening of the C–O distance. The triangle of Rh atoms that contains the substituted Rh atom, with the substituent projecting above that triangle, shows a pronounced lengthening of the Rh–Rh bonds *cis* to the heteroligand. There is an equally pronounced shortening of the Rh–Rh bond across the triangle from the substituted Rh atom. A third effect is the displacement of the CO groups in triply bridged Rh_3 triangles containing the RhL moiety, so that they almost doubly bridge the two Rh–Rh bonds *cis* to the substituted Rh atom. Although no clear correlations exist within this group of substituents the localized effects can generally be associated with an increase of electron density on the substituted Rh atom. The other monosubstituted clusters that contain quite different neutral and anionic heteroligands do not display common trends in the structural distortions induced by the substituents, and this is evidently due to the very varied nature of the ligands within this group.

Introduction

Rhodium carbonyl complexes, including cluster compounds, are widely used as catalysts for various organic reactions,^{1,2} particularly important examples of which are carbonylation, hydrogenation and oxidation processes. It is also well known that substitution of CO in binary carbonyl complexes by heteroligands, such as P donors, can substantially change their reactivity and catalytic activity.³ Recent studies have demonstrated the effect of labile ligands on the substitution kinetics of the $\text{Rh}_6(\text{CO})_{15}\text{L}$ clusters ($\text{L} = \text{Me}_2\text{SO}$, MeCN , C_8H_{14} , THF or EtOH)⁴ and the influence of P-donor substituents on the reactivity⁵ and ligand sphere dynamic processes⁶ in substituted derivatives of $\text{Rh}_6(\text{CO})_{16}$. These dynamic characteristics (kinetics and stereochemical non-rigidity) depend on both ground and transition state properties of the molecules under study. Structural information is an important part of molecular ground state characteristics and studies of structural distortions originating from a heteroligand substituted into the coordination sphere can provide a basic insight into dynamic manifestations of ligand effects. Such studies are also important in revealing the extent to which substituent effects are dissipated evenly throughout the cluster as a whole or, rather, if they are concentrated in the vicinity of the substituent. These distinctions should provide insight into how the electron densities within the molecular orbitals respond to substituents in general or specifically to substituents of particular types.

Several $\text{Rh}_6(\text{CO})_{15}\text{L}$ derivatives ($\text{L} = \text{SMe}_2$,^{7a} PPh_3 ,^{7b} VinPy ($\text{VinPy} = 4\text{-vinylpyridine}$),^{7c} COEt^- ,^{7d} CO_2Me^- ,^{7d} I^- ,^{7e} Cl^-)^{7f} have already been synthesized and structurally characterized but these contain very different heteroligands and this prevents a systematic approach to the data interpretation. In the present paper structures of nine $\text{Rh}_6(\text{CO})_{15}\text{L}$ derivatives, with $\text{L} = \text{P}(\text{OPh})_3$ (**1**), $\text{P}(4\text{-XC}_6\text{H}_4)_3$ ($\text{X} = \text{CF}_3$, **2**; Cl , **3**; F , **4**; OMe , **5**), $\text{P}(\text{tBu})_3$ (**6**), Me_2SO (**7**), MeCN (**8**), and C_8H_{14} (**9**), are reported and some typical features of structural ligand effects are discussed. Redetermination of the $\text{Rh}_6(\text{CO})_{16}$ structure has also been performed to provide data of improved accuracy for the parent cluster as compared with those obtained^{7g} more than 30 years ago.

Experimental

Chemicals

Dichloromethane (CH_2Cl_2) and dimethyl sulfoxide (DMSO) were used as received. Acetonitrile was refluxed for 5 h over P_2O_5 and then distilled over a fresh portion of the drying agent. Cyclooctene (Aldrich) was distilled and the fraction that came over at 143–145 °C was stored under argon. $\text{P}(\text{tBu})_3$ was distilled under reduced pressure of argon immediately before use. $\text{P}(\text{OPh})_3$, $\text{P}(4\text{-F}_3\text{CC}_6\text{H}_4)_3$, $\text{P}(4\text{-FC}_6\text{H}_4)_3$, $\text{P}(4\text{-ClC}_6\text{H}_4)_3$ and $\text{P}(4\text{-MeOC}_6\text{H}_4)_3$ were used as received.

Synthesis of the $\text{Rh}_6(\text{CO})_{15}\text{L}$ clusters

The parent $\text{Rh}_6(\text{CO})_{16}$ cluster (**10**) and its acetonitrile derivative (**8**) were prepared as described earlier.⁸

[†] Electronic supplementary information (ESI) available: synthesis conditions, IR data, crystal data, bond lengths and angles, ORTEP views of the clusters. See <http://www.rsc.org/suppdata/dt/b0/b010109p/>

The substituted derivatives (**1–6**) containing the P-donor ligands $L = \text{P}(\text{OPh})_3$ (**1**), $\text{P}(4\text{-XC}_6\text{H}_4)_3$ ($\text{X} = \text{CF}_3$, **2**; Cl , **3**; F , **4**; MeO , **5**), and P^iBu_3 (**6**) were prepared by the substitution of acetonitrile in **8** in the presence of a slight (1.1 to 5 fold) excess of the corresponding nucleophile in CH_2Cl_2 . The products were separated using column chromatography: silica 5–40 mesh, eluent hexane–dichloromethane. Yields, eluent compositions, conditions of crystallization, and IR characteristics of the clusters **1–6** are given in the electronic supplementary information (ESI).

Clusters with $L = \text{Me}_2\text{SO}$ (**7**) and cyclooctene (**9**) were synthesized by acetonitrile ligand replacement in the presence of large excesses of the substituting ligands. Addition of hexane to the reaction mixture and concentration of the solution under reduced pressure results in precipitation of the final products in 90–95% yield. Conditions of crystallization of these clusters are included in the ESI together with their IR absorption bands in the C–O stretching region.

Data collection, solution and refinement for **1–10**

Data for the crystal structure analysis of compounds **1–10** are given in the ESI. For **1**, **4**, **7**, **8** and **9** data were collected on a Siemens P4 diffractometer and for **2**, **3**, **5**, **6** and **10** data were acquired on a Nonius Kappa CCD diffractometer. All data were collected at or below 173 K. For compounds **2**, **3**, **5**, **6** and **10** the data frames were integrated and scaled using the Denzo-SMN package.⁹ They were corrected for absorption effects by their program which uses the high redundancy of the data to apply a scale to each frame collected.

The structures were solved by direct methods using SHELXTL PC Release 4.1.¹⁰ Refinement was by full-matrix least-squares calculations on F^2 with anisotropic thermal parameters for all non-H atoms. Data for compounds **1**, **4**, **7**, **8** and **9** were corrected for absorption using the program SHELXA.¹¹

Selected structural parameters for the molecules are listed in the ESI, as are ORTEP¹² views of **1**, **9** and **10**. All calculations were carried out using the program SHELXTL PC Release 4.1.^{10,13}

CCDC reference numbers 163529–163538.

See <http://www.rsc.org/suppdata/dt/b0/b010109p/> for crystallographic data in CIF or other electronic format.

Results

General considerations

The molecule of the parent $\text{Rh}_6(\text{CO})_{16}$ cluster consists of an octahedral hexanuclear core surrounded by four triply bridging CO ligands which occupy the four opposite faces of the octahedron. Twelve terminal ligands are symmetrically distributed over six metal atoms, two at each one. The molecule belongs to the idealized T_d symmetry point group that makes all the bridging carbonyl groups equivalent, as well as all terminal carbonyl groups and all the rhodium atoms. The same is true for the structural parameters such as Rh–Rh bond lengths, and for the characteristics of the corresponding fragments made up by the terminal and bridging Rh–CO groups. This high degree of symmetry makes the molecule particularly convenient for the study of various manifestations of ligand effects arising when a CO group is replaced by a ligand with different electronic and/or steric properties. From the structural viewpoint, each particular feature of the structural distortions of a substituted cluster should, in principle, be assignable to the electronic and/or steric effects induced by the heteroligand relative to the equivalent molecular characteristics in the starting compound.

The molecules of the $\text{Rh}_6(\text{CO})_{15}\text{L}$ derivatives, as shown by the example in Fig. 1, contain Rh_6 octahedra essentially similar to that found in the parent $\text{Rh}_6(\text{CO})_{16}$ cluster. The ligand

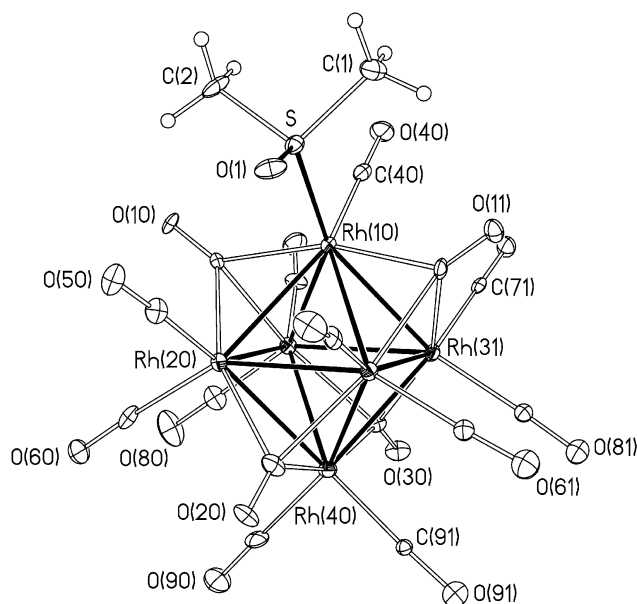


Fig. 1 ORTEP view of the $\text{Rh}_6(\text{CO})_{15}(\text{DMSO})$ cluster.

environment contains four triply bridging CO groups and ten terminal CO ligands occupying two terminal sites on each of the five unsubstituted Rh atoms. The two coordination sites on the sixth rhodium atom (Rh(10) in Fig. 1) are occupied by the eleventh terminal CO and the heteroligand, which is bonded to Rh(10) in an η^1 mode for the clusters **1–8**. The cyclooctene in derivative **9** is coordinated in an η^2 mode, and the DMSO ligand in **7** is coordinated to Rh(10) through the sulfur atom.

Although the groups attached to the P-donor atoms do seem to display some regular conformational arrangements these are clearly properties of the solid state since no inequivalent phenyl rings, for example, were ever observed in NMR spectra.

All the clusters belong to the idealized C_s symmetry group and the analysis of the heteroligand effect will be made under the framework of this idealized representation. For the sake of simplicity the atom numbering scheme shown in Fig. 1 is simplified (in the ESI and text) by omitting the second figure in the numbers. This second figure, 0 or 1, is there to differentiate atoms that are distinguishable in crystallographic analysis but which can be considered equivalent in terms of the idealized C_s symmetry group of the molecules. Therefore these second figures are not of importance for the general analysis to be performed. Selected structural parameters of the molecules **1–9** are presented in the ESI. To involve as many data as possible in the analysis of the ligand effects the structural parameters of analogous monosubstituted derivatives characterized earlier⁷ are given in the ESI as well.

Substitution of a heteroligand into the coordination sphere of the $\text{Rh}_6(\text{CO})_{16}$ cluster results in distortions of the core geometry along with changes in the structural parameters of coordinated CO groups. In general, and in accordance with what would be expected from an increase in average electron density on the Rh_6 core, the substituent induces a decrease in the average Rh–CO bond length and an increase in the average C–O bond length. However, these changes are small compared with the standard deviations of the reference bond lengths. The averages of the Rh–(μ_3 -CO) bond lengths are actually increased slightly by the presence of the substituent but again the effects are small. Similarly, the average of the Rh–Rh bond lengths in a given cluster is very nearly always longer than that in $\text{Rh}_6(\text{CO})_{16}$ but very seldom by more than the standard deviation of the average in the substituted cluster. In all these cases the averages conceal quite wide variations in individual bond lengths within a particular cluster. Although it is not always the same pair of bond lengths that are longest and shortest, the ranges of the Rh–Rh bond lengths in all the clusters average 76(8) pm. (The

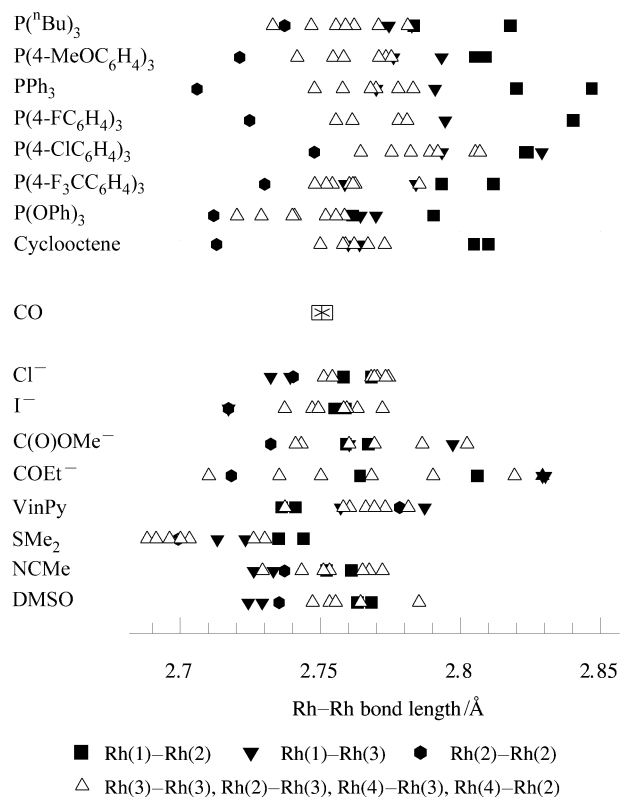


Fig. 2 Rh–Rh bond lengths in monosubstituted $\text{Rh}_6(\text{CO})_{15}\text{L}$ derivatives.

uncertainties here and elsewhere are estimated standard deviations of the averages.) The ranges of the Rh–(CO) bond lengths average 69(6) pm (omitting $\text{L} = \text{NCMe}$ and I^- which show unusual features) and the ranges of the Rh–(μ_3 -CO) bonds are even larger, the average for all the clusters being 153(9) pm. These observations suggest that a careful examination of the substituent effects on particular bonds might show how the effects are distributed around the clusters and whether the effects are stereoselective or not. To aid in this analysis the data are represented diagrammatically in Figs. 2 and 3, where corresponding bonds are symbolized by the same “bullets”.

The Rh–Rh bonds

Analysis of the general trends in the Rh–Rh distances in the Rh_6 octahedron (Fig. 2) shows that the substituted clusters can be divided into two groups. Group 1 comprises the clusters with P-donor ligands and cyclooctene. All of these display similar, quite large and systematic geometrical changes in the cluster skeletons that can undoubtedly be ascribed to the effect of the heteroligands. Group 2 consists of the clusters containing a variety of rather disparate neutral and anionic ligands where the distortions from octahedral geometry are sometimes also quite large but not systematic.

Group 1. Within this group the average values of the Rh–Rh bond lengths vary from 2.75(2) Å ($\text{L} = \text{P}(\text{OPh})_3$) to 2.79(2) Å ($\text{L} = \text{P}(4\text{-ClC}_6\text{H}_4)_3$). Apart from the cluster containing the $\text{P}(\text{OPh})_3$ substituent (the only π -acid ligand used) there is a general elongation of the bonds of up to 44 pm as compared with the 2.75(1) Å in the parent cluster. However, in all these clusters the shortest bond is between the two Rh(2) atoms and the longest is between Rh(1) and Rh(2) so the substituent effect is quite stereospecific. The difference between the long and short bonds rises to 141 pm for the $\text{Rh}_6(\text{CO})_{15}(\text{PPh}_3)$ cluster, with the average range being 95(8) pm. Thus the data given in Fig. 2 show unambiguously that the two bonds between the substituted Rh(1) atom and the two Rh atoms in the equatorial

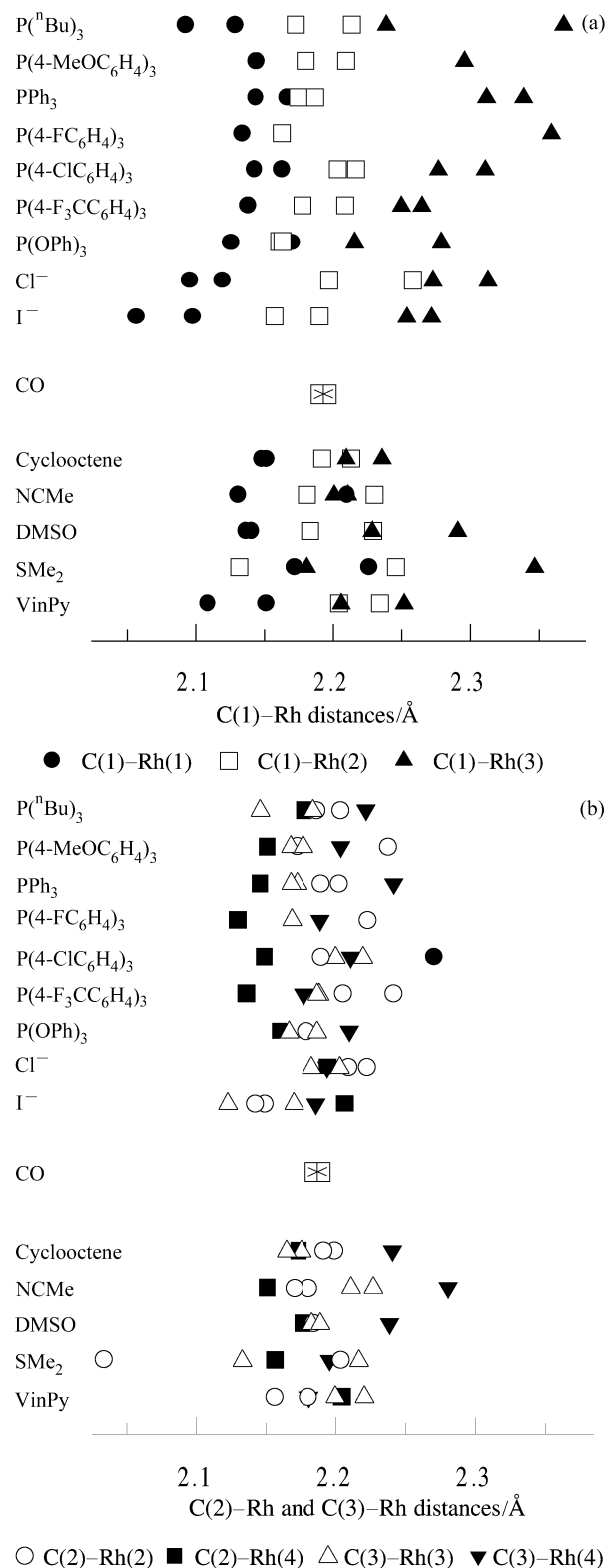


Fig. 3 Rh–(CO) bond lengths in monosubstituted $\text{Rh}_6(\text{CO})_{15}\text{L}$ derivatives.

plane that are *cis* to the substituent are the longest ones in all but one of the eight clusters under consideration. The Rh(1)–Rh(3) bonds, which are *trans* with respect to the heteroligand, are the second longest, being on average only 30(5) pm shorter than the average Rh(1)–Rh(2) bond, but they are still *ca.* 30(5) pm longer than the average of 2.750 Å for the Rh–Rh bonds in $\text{Rh}_6(\text{CO})_{16}$.

The position of the shortest Rh–Rh bond in the octahedron in all Group 1 clusters also demonstrates stereoselectivity. Apart from the very slight exception of the P^nBu_3 cluster,

the Rh(2)–Rh(2) bonds are always the shortest. The rest of the metal–metal bonds in the octahedron are grouped around the corresponding average value without significant deviations from it. Thus, the ligand effect is displayed in the vicinity of the substituent and consists both in elongation of the nearest Rh–Rh bonds and contraction of the Rh(2)–Rh(2) bonds disposed in the equatorial plane of the octahedron.

Although the Rh(2)–Rh(2) bonds are almost always the shortest they do not show any regular trend with respect to the sigma donicity of the donor P-ligands. Similarly no regular trend with P-donor basicity is shown for the (longest) Rh(1)–Rh(2) bonds.

Group 2. The clusters that fall into this group contain quite different substituting ligands, and there are no systematic trends in the ligand effects. It is perhaps worthwhile to mention that in two halide derivatives the Rh(1)–Rh(3) metal–metal bonds are the shortest, *i.e.* the ones *trans* with respect to the heteroligand, and the longest distances were found for the Rh(2)–Rh(3) bonds, again in contrast to Group 1 compounds.

Rh–(μ_3 -CO) and μ_3 -C–O bonds

The bonding of the triply bridging carbonyls shows even more distortion from the high symmetry found in Rh₆(CO)₁₆ than the distortions from octahedral symmetry shown by the Rh₆ core. The distortions are shown clearly in Fig. 3 and the clusters can again be divided into two groups. As before, the first one includes the P-donors, but now the two halide derivatives can be included as well. The general feature of the structure of these clusters that puts them together is a pronounced distortion in the coordination mode of the triply bridging C(1)O groups adjacent to the heteroligand. The heteroligand effect in this case consists in a shift of both the bridging COs from the idealized position over the centre of the Rh(1)–Rh(2)–Rh(3) triangles. This shift consists in a movement towards becoming doubly bridged with respect to the Rh(1)–Rh(2) bonds, in spite of the fact that the Rh(1)–Rh(2) bonds are generally the longest in these clusters. Thus, one can easily observe a major contraction of the Rh(1)–C(1) bonds, almost no change in the Rh(2)–C(1) bonds, and considerable elongation of the Rh(3)–C(1) bonds, the averages of the 18 bond lengths in each case being 2.129(8), 2.188(7) and 2.292(17) Å, respectively, compared with the average of 2.186(4) Å in Rh₆(CO)₁₆. The first and the last bonds are respectively the shortest and longest in virtually all the individual molecules of both groups (Fig. 3).

The two other bridging ligands, C(2)O and C(3)O, are distinguished from each other, respectively, by their bridging the Rh₃ triangles that include the Rh(2) and Rh(3) atoms and they are different in their positioning with respect to the substituent. They are disposed in parts of the Rh₆ octahedron remote from the substituent and do not display any systematic distortions in their coordination apart from the fact that the C(2)–Rh(4) are generally shorter than the C(3)–Rh(4) bonds. This points again to the essentially local character of the heteroligand effect.

In contrast to the structural distortions observed for the Rh–C bonds, the data available in the ESI show that the C–O bonds for bridging carbonyl groups do not display any systematic trends in their changes as compared with the parent Rh₆(CO)₁₆ cluster. The biggest spread of the C–O distances for a particular molecule has been found for the SMe₂ derivative where it is 75 pm, whereas for the other clusters this difference in general does not exceed 30–40 pm. The average values of the bridging C–O bond lengths are grouped around the corresponding value found in Rh₆(CO)₁₆, 1.153(6) Å, ranging from 1.136(27) (SMe₂) to 1.194(12) Å (I[–]), the spread for the P-donor ligands being smaller (1.147 to 1.179 Å).

Terminal CO groups

The average bond lengths in the Rh–C–O terminal fragments

of the substituted clusters in general display slight contraction of the Rh–C distances (but only by 19 pm with respect to the average Rh–CO distance of 1.915(15) Å in Rh₆(CO)₁₆) and an even smaller elongation of the C–O bonds (6 pm as compared with the average of 1.126(13) Å in Rh₆(CO)₁₆). This general but small contraction of all the terminal Rh–CO bonds contrasts with a quite significant specific contraction of the Rh(1)–C(4) bonds. Thus, apart from the NCMe cluster where the bond is actually lengthened by 20 pm, the Rh(1)–C(4) bonds are an average of 52(4) pm shorter than the corresponding average distance of 1.915 Å in Rh₆(CO)₁₆. Also (apart from the NCMe, iodide and SMe₂ clusters where the bonds are shortened by 44, 6 and 13 pm respectively), the C(4)–O bonds are an average of 18(4) pm longer than the average C–O bond in Rh₆(CO)₁₆, a smaller and statistically less pronounced effect.

Other terminal CO groups do not exhibit significant variations from the average value and this emphasizes again the essentially short distance or local nature of the substituent effect. The cluster that shows major deviations from these trends is the acetonitrile derivative where the heteroligand causes a quite large increase of 20 pm in the Rh(1)–C(4) bond and a 44 pm decrease in the C(4)–O bond.

Rh–P bonds

The lengths of the Rh–P bonds cover a range of 130 pm and the average length (2.364(6) Å) of the bonds in the clusters that contain the isosteric substituents P(4-XC₆H₄)₃ (Tolman cone angle, θ , = 145°) is 20 pm longer than the Rh–P(^{*i*}Bu)₃ bond and 113 pm longer than the Rh–P(OPh)₃ bond. P(^{*i*}Bu)₃ and P(OPh)₃ have similar cone angles (132 and 128°, respectively), but P(^{*i*}Bu)₃ is the most effective net electron donor, and P(OPh)₃ the least effective, of all the P-donors involved.

Discussion

The effects of substituents on the overall structures and detailed dimensions of metal carbonyl clusters are important in indicating whether there is a “ground state rationale” for observed trends in reactivity, and whether these effects are dissipated throughout the cluster as a whole or concentrated in specific regions of it. Complementary structural and dynamic studies involving substituents that vary systematically in their electronic and steric natures are still quite rare but the advent of CCD diffractometers, with their capacity to provide crystal structures in astonishingly short times, seems likely to make the structural studies much more common. The study of molecular dynamics through NMR spectroscopy has also progressed technologically quite rapidly in recent years and systematic relationships between those dynamics and corresponding structures have been observed recently⁶ and seem likely to be found increasingly in the near future. Unfortunately, no such increase in the rate of production of kinetic data seems technologically likely although a greater interest in making kinetic measurements may be stimulated by the structural data.

Some detailed relationships between structural and kinetic effects of substituents have, however, been observed. For example, the tendency of the clusters M₃(CO)_{12–n}L_n (M = Ru or Os; L = a P-donor ligand and *n* = 0–3) to undergo bimolecular fragmentation (Fn2) reactions, induced by P-donor nucleophiles, is greatly enhanced when *n* = 1,^{14,15} and the M–M bond lengths that are *cis* to the substituents are significantly lengthened in those clusters.¹⁶

The new structures reported here show that there are effects that are due particularly, though not exclusively, to the P-donor substituents, and that are dispersed over the cluster as a whole. This is shown by the lengthening of the average Rh–Rh bond lengths and the shortening and lengthening of the Rh–CO and RhC–O bonds, respectively. The latter are what are expected from an increase in electron density in the cluster due to the

more electron donating substituent, and the lengthening of the average Rh–Rh bonds suggests that the increase of electron density takes place in Rh₆ antibonding orbitals. The lengthening of the RhC–O bonds is also in accord with the general decrease in the $\nu(\text{CO})$ stretching frequencies of the strongest bands observed in the clusters (ESI).

However, these effects are all quite small and are dwarfed by much more significant effects that are localized in the neighbourhood of the substituents. These show up, in each cluster, in several ways.

(i) The shortening of the Rh–CO bond, and the corresponding lengthening of the RhC–O bond, in the CO ligand that is bonded to the same Rh atom as the substituent.

(ii) The lengthening of the two Rh–Rh bonds that are *cis* to the substituent and that are in the Rh₃ triangular face above which the substituent lies.

(iii) The lengthening, but to a lesser extent, of the two Rh–Rh bonds that are *trans* to the substituent.

(iv) The shortening of the Rh–Rh bond that lies across the previously mentioned Rh₃ face from the substituent.

(v) The movement of the two triply bridging CO ligands that lie over two opposite Rh₃ faces that include the substituted Rh atom so that they essentially doubly bridge the two long Rh–Rh bonds *cis* to the substituted Rh (see ii above). This movement is naturally coupled with quite large changes in the Rh–(μ_3 -CO) bond lengths.

Observation (i) is fully in accord with a simple electronic effect caused by the greater electron donicity of the P-donors as a whole. The dependence of the shortening of the Rh–(CO) bond on the nature of the P-donor is not particularly pronounced, there being no trend with P-donor basicity among the clusters containing the isosteric P(4- XC_6H_4)₃ ligands. However, the longest bond is the one associated with the weakest donor phosphine and the most donating phosphine has the second shortest bond.

The lengthening of the Rh–Rh bonds *cis* to the substituent is reminiscent of the corresponding lengthening observed in the clusters Ru₃(CO)₁₁L¹⁶ and Ru₅C(CO)₁₄L,¹⁷ where L is also a group of P-donor substituents. In those cases there seems¹⁷ to be a small, statistically significant trend in which the bond lengths increase slightly with increasing size and/or basicity of the substituent. However, other effects, possibly due to crystal packing, are more important, and Fig. 2 shows that there is no clearly rationalizable trend shown by the *cis* Rh–Rh bond lengths in the Rh₆ clusters.

A clear feature of the data for the Ru₃(CO)₁₁L and Ru₅-C(CO)₁₄L complexes was a highly significant trend of increasing Ru–P bond lengths with increasing donicity and/or size of the substituents.¹⁶ These two effects could not be separated because of the correlation between the size and donicity of the P-donors used. No clear trend with basicity is shown by the Rh–P bond lengths in the Rh₆ clusters containing the isosteric P(4- XC_6H_4)₃ substituents.

However, the Rh–P(^{*n*}Bu)₃ bond is considerably longer than the Rh–P(OPh)₃, indicating an increase in Rh–P bond length with increasing net donicity of the two similarly sized ligands. This trend, the possible existence of which has been indicated previously,¹⁶ is, of course, counterintuitive. One would have expected bond strengths to increase, and bond lengths to decrease, with increasing basicity. The generally greater lengths of the Rh–P(4- XC_6H_4)₃ bonds is in accord with the greater size of the ligands involved, and this possible steric effect is also indicated by the instability that we find for the PCy₃ derivative with its very much larger ligand ($\theta = 178^\circ$).

While all these observations should possibly be rationalized in terms of some sort of bonding model we do not think it profitable to speculate about this yet. We prefer rather to wait for data for clusters that contain a larger group of substituents, with more varied electronic and steric properties, and for the outcome of possible Density Functional Theory calculations.

Note added in proof: We have recently become aware of the paper by Professor Pomeroy *et al.* (K. Biraha, V. M. Hansen, W. K. Leong, R. K. Pomeroy and M. J. Zaworotko, *J. Cluster Sci.*, 2000, **11**, 285) where they report results of a structural study of a number of clusters Os₃(CO)₁₁L (L = P donor ligand) which show some similar features to those reported here.

Acknowledgements

We thank the Natural Sciences and Engineering Research Council of Canada, the NATO (Grant OTR.CRG 951482), and the Competitive Centre in Natural Science (Russia), for financial support. E.V.G. also appreciates the award of a scholarship (Grant No M99-2.5K-128) from the Foundation for Basic Researches (St. Petersburg University).

References

- 1 G. W. Parshall and S. D. Ittel, *Homogeneous Catalysis*, Wiley, New York, 2nd edn., 1992; D. F. Shriver, P. Atkins and C. H. Langford, *Inorganic Chemistry*, W. H. Freeman, New York, 2nd edn., 1994; W. L. Gladfelter and K. J. Roesselet, in *The Chemistry of Metal Cluster Complexes*, eds. D. F. Shriver, H. D. Kaesz and R. D. Adams, VCH, New York, 1995, ch. 7.
- 2 R. S. Dickson, *Homogeneous Catalysis with Complexes of Rhodium and Iridium*, Reidel, Dordrecht, 1985; G. Süss-Fink and G. Meister, *Adv. Organomet. Chem.*, 1993, **35**, 41.
- 3 M. Castiglioni, R. Giordano and E. Sappa, *J. Organomet. Chem.*, 1988, **342**, 111.
- 4 A. J. Poë and S. P. Tunik, *Inorg. Chim. Acta*, 1998, **268**, 189.
- 5 I. O. Koshevoy, A. J. Poë and S. P. Tunik, manuscript in preparation.
- 6 S. P. Tunik, I. S. Podkorytov, B. T. Heaton, J. A. Iggo and J. Sampanthar, *J. Organomet. Chem.*, 1998, **550**, 221; E. V. Grachova B. T. Heaton J. A. Iggo I. S. Podkorytov, D. J. Smawfield, S. P. Tunik and R. Whyman, manuscript in preparation.
- 7 (a) S. Rossi, K. Kallinen, J. Pursiainen, T. T. Pakkanen and T. A. Pakkanen, *J. Organomet. Chem.*, 1991, **419**, 219; (b) S. P. Tunik, A. V. Vlasov, N. I. Gorshkov, G. L. Starova, A. B. Nikol'skii, M. I. Rybinskaya, A. S. Batsanov and Yu. T. Struchkov, *J. Organomet. Chem.*, 1992, **433**, 189; (c) S. P. Tunik, S. I. Pomogailo, G. Dzhardimalieva, A. D. Pomogailo, I. I. Chuev, S. M. Aldoshin and A. B. Nikol'skii, *Russ. Chem. Bull.*, 1993, **42**, 937; (d) G. Ciani, A. Sironi, P. Chini and S. Martinengo, *J. Organomet. Chem.*, 1981, **213**, C37; (e) V. G. Albano, P. L. Bellon and M. Sansoni, *J. Chem. Soc. A*, 1971, 678; (f) A. L. Rheingold, C. B. White, P. D. Macklin and G. L. Geoffroy, *Acta Crystallogr., Sect. C*, 1993, **49**, 80; (g) E. R. Corey, L. F. Dahl and W. Beck, *J. Am. Chem. Soc.*, 1963, **85**, 1202.
- 8 S. P. Tunik, A. V. Vlasov and V. V. Krivykh, *Inorg. Synth.*, 1996, **31**, 239.
- 9 Z. Otwinowski and W. Minor, *Methods Enzymol.*, 1977, **276**, 307.
- 10 SHELXTL PC Release 4.1, Siemens Analytical X-Ray Instruments Inc., Madison, WI, 1990.
- 11 G. M. Sheldrick, SHELXA, University of Göttingen, 1990.
- 12 C. K. Johnson, ORTEP II, Report ORNL-5138, Oak Ridge National Laboratory, Oak Ridge, TN, 1976.
- 13 *International Tables of Crystallography*, Kynoch Press, Birmingham, 1969, vol. 4.
- 14 N. M. J. Brodie, A. J. Poë and V. Sekhar, *J. Chem. Soc., Chem. Commun.*, 1985, 1090; A. J. Poë and V. Sekhar, *Inorg. Chem.*, 1985, **24**, 4376; N. M. J. Brodie and A. J. Poë, *Inorg. Chem.*, 1988, **27**, 3156.
- 15 L. Chen and A. J. Poë, *Coord. Chem. Rev.*, 1995, **143**, 265.
- 16 N. M. J. Brodie, L. Chen, A. J. Poë and J. F. Sawyer, *Acta Crystallogr., Sect. C*, 1989, **45**, 1314.
- 17 R. A. Burrow, D. H. Farrar, J. Hao, A. Lough, O. Mourad, A. J. Poë and Y. Zheng, *Polyhedron*, 1998, **17**, 2907.